Iraqi National Journal of Earth Science, Vol. 26, No. 04, 2026 (01-18)

Iraqi National Journal of Earth Science

www.earth.uomosul.edu.iq

Paragenesis and Multi-fracture System in Jurassic Barsarin Formation: Implications from Various Burial Settings, NE-Iraq

Rayan Fattah [1], **Namam Salih** [2*], **Alain Préat** [3]

rayanmhamadfatah99@gmail.com namam.salih@soran.edu.iq alain.preat@ulb.be

[1] *Department of Petroleum Geosciences, Science Faculty, Soran University, Erbil, Soran-44008, Iraq*
[2] *Department of Petroleum Engineering and Mining, Engineering Faculty, Soran University, Soran-Erbil, 44008, Iraq*
[3] *Res. Grp., Biogeochemistry and Modelling of the Earth System, Université Libre de Bruxelles, 1050 Brussels, Belgium*
[*] *Corresponding author*

Received: 23 January 2025 Received in revised form: 20 March 2025 Accepted: 13 May 2025
Available online: 01 October 2026

Abstract

Generation of fracture systems and geofluid evolution in shallow and subsurface environmental conditions play a critical role in various geological processes and petroleum applications. This paper evaluates comprehensive data to provide a deep understanding of multi-fracturing systems dissolved/filled by various cement phases related to different tectonic settings and the influx of diagenetic fluids in near-surface and subsurface settings. This study utilized intensive field observation and an optical microscope to track the paragenesis of the targeted formation and fracture stages in the Jurassic interval. The study recognizes five main types of fractures: (1) FI generated during surface or near surface conditions; the timing of initiating FI is not older than low-amplitude stylolite (LAS) (2) FII formed in shallow burial diagenesis and was coeval with late diagenetic stage, (3) FIII in-situ fractures formed in the subsurface conditions coinciding with high-amplitude stylolitization (HAS), (4) FIV fracture filled by calcite cement with plenty of solid bitumen fluid inclusions; and (5) FV-filled dolomite cements. The characteristics and appearance of dolomite crystals, corrosion, suture contact between saddle dolomite/calcite grains, and tightly compacted grains are directly linked to the increasing burial weight of overlying sedimentary rocks during the "Mesogenesis Phase". In summary, the findings add new insight as the fractures act as essential conduits and barriers in hydrocarbon migration and accumulation through various geological processes, from their formation during deposition to their evolution and the fracturing significant in post-depositional settings. The recognition of how these fractures originated enables more effective exploration and production strategies in hydrocarbon reservoirs.

Keywords:

Fracturing; Petrography; Dolomitization; Upper Jurassic Carbonate rocks; Stylolitization; Paleo-fluids Evolution; Shallow and deep-burial diagenesis.

DOI: 10.33899/injes.v26i4.60916, ©Authors, 2026, College of Science, University of Mosul.
This is an open-access article under the CC BY 4.0 license (http://creativecommons.org/licenses/by/4.0/).

==========

1. Introduction

Fractures show mechanical failures of the rock strength to natural geological stresses such as tectonic movement, lithostatic pressure variations, thermal stresses, high fluid pressure, and even fluid withdrawal, since fluid also partially supports the weight of the overburden rock (Tiab and Donaldson, 2003). Fractures are essential for hydrocarbon storage and act as conduits for fluid flow (Xu et al., 2016; Peacock et al., 2016). Fractures are recognized as significant migration paths for hydrothermal fluids, which contribute to the formation of saddle dolomite (Tiab and Donaldson, 2033) and hydrothermal dolostone reservoirs (Zhao et al., 2012; Jiang et al., 2016). Fracture effectiveness often refers to the condition when natural fractures are open, facilitating efficient fluid flow under reservoir conditions (Lu et al., 2018; Oyedokun and Schubert, 2017). The effectiveness of fractures can be analyzed by examining the filling time of paleo-fluid, the period of fracture development, the time of cement breaking, and the subsequent dissolving time (Ren et al., 2019; Amirjan and Bozorg, 2018). Natural fractures can substantially influence the flow of

formation and production fluids, particularly in low-permeability rock formations (Weisenberger et al., 2019). They establish conduits between organic-rich source layers and matrix pores during hydrocarbon charging, as well as between matrix pores, hydraulic fractures, and the wellbore during extraction (Warpinski and Lorenz, 2008).

The presence of cement in fractures, whether cemented or cement-lined, along with the topology of fracture cement and porosity, can greatly affect fracture permeability, impacting well productivity and reservoir performance (Landry et al., 2016, Wennberg et al., 2016). The diagenetic condition of cracks may affect fluid flow on a basin scale (Fischer et al., 2009, Bjørlykke and Jahren, 2012). The kind and quantity of fracture cement can impact fracture spacing (Hooker and Katz, 2015)and**,** among other variables, cement in pre-existing fractures can influence subsequent fracture propagation (Virgo et al., 2014, Lee et al., 2018). Comprehending the mechanisms of cement accumulation in fractures is crucial for forecasting the flow and storage characteristics of these rocks (Weisenberger et al., 2019). Cements convey insights into the physical and chemical conditions of the reservoir during various diagenetic stages, as well as fluid composition, so yielding information that would otherwise be inaccessible from voids (Baqués et al., 2020). Significant variables influencing the diagenesis of carbonate rocks include fluctuations in sea levels linked to tectonic events and climatic variations, as well as sedimentary diagenesis (Bathurst, 1972). Therefore, the rocks rapidly respond to diagenetic processes such as cementation, dissolution, porosity, and neomorphism that lead to the destruction of the sedimentary textures, skeletal grains, and groundmass (Boggs, 2006). Compaction is a detrimental factor in carbonate rocks, resulting from significant lithostatic pressure, which decreases porosity (Rasool et al., 2023). Dissolution can also occur due to meteoric and organic acids, as well as high-temperature and magnesium-rich fluids (Baqués et al., 2020). Dissolution surfaces and stylolites are generated due to pressure solution (Jiayu, 1999). Stylolites arise from heightened overburden sedimentation or tectonic pressure, influencing the grains in carbonate rock, facilitating disintegration, and extending seams (André et al., 2010). Dolomitization is a significant diagenetic event in the Jurassic strata and **is** characterized by broad and pervasive dolomitization exhibiting various crystal sizes (Rasool et al., 2023).

Numerous natural fractures that developed under moderate to profound burial conditions throughout geological time scales are lined or sealed with mineral cement (Laubach, 2003). The extent of fill is influenced by the fracture size, the rate of fracture opening, heat exposure, geochemical conditions, and the reactivity and composition of the fracture-vertical rock formations (Lander and Laubach, 2014). Therefore, several scholars have studied the timing and generation of fracture systems based on the geometry of the rock, paragenesis, and staging of fractures by cross-cutting or direct dating using U-Pb radiogenic isotopes (Salih et al., 2019a, Shen et al., 2019, Shen et al., 2022, Xu et al., 2025).

During the deposition phase, the mechanical properties of sediment are influenced by the accumulation of layers, leading to load-induced fracturing. This is evident in carbonate systems, where the early cementation of sediments can generate stress within the sediment column, resulting in brittle fracturing. For instance, McNeill and Eberli (2009) observed that the rapid progradation of carbonate margins can lead to early fracturing due to the load from overlying sediments (McNeill and Eberli, 2009). The presence of different cement types, such as dolomite or calcite, in these fractures further complicates the interaction between deposition and fracturing, influencing fluid pathways critical for diagenetic processes, as shown by (Budd et al., 2013).

In a syn-depositional environment, fractures can serve as conduits for fluid movement and chemical exchanges, significantly affecting the diagenetic evolution of the sediments. For example, syn-depositional fractures in high-relief carbonate platforms can facilitate the migration of diagenetic fluids, enhancing the permeability of these structures (Berra and Carminati, 2012). Studies by Léveillé et al. (2014) suggested that cements can fill fractures during this stage, which provides insights into past aqueous activity (Léveillé et al., 2014). These can effectively alter reservoir characteristics by influencing mineral precipitation and fluid dynamics during the early stages of sedimentary formation.

Furthermore, the fracturing system during post-deposition continues to evolve the interaction between fractures and cementation, with existing

fractures potentially sealed by subsequent cementation, altering flow pathways through the rock. Fracturing often precedes or coincides with cementation processes, with fracture fills affecting the mechanical integrity of the rock and consequently its reservoir quality. Gale et al. (2004) noted that the characteristics of dolostone reservoirs can reflect the geological interplay between fracturing and the growth of cements that seal these fractures (Gale et al., 2004). The timing of fracture growth relative to cementation is vital, as it determines how fractures accommodate fluid migration within the diagenetic landscape (Salomon et al., 2020). Moreover, the type and degree of cementation are influenced by several factors, including sedimentology, the chemical composition of pore fluids, and mechanical stability. The distribution of fractures is not uniform and can depend on lithology and other sedimentologic characteristics, suggesting a predictive model for understanding fracture networks based on these controls (Sonntag et al., 2014).

Therefore, in carbonate systems, the mechanical and diagenetic interactions show that the observed fractures can provide significant insights into past sedimentary environments and tectonic activities, which is valuable for hydrocarbon exploration and other geological applications. However, there is not enough data about the timing of the fracture system based on the type of cementation that originated from various paleo-fluid sources. Therefore, the novelty of this work is to understand the timing and staging of the fracture system within the Upper Jurassic formation based on the type of cement that requires not less than 1Ma to accumulate inside the pore spaces of these fractures.

2. Aims and objectives of the study area

The main aim and objective of this work is to conduct an in-depth investigation and analysis of the fracture systems that are produced from the source rocks of the Barsarin Formation, with a particular emphasis on understanding their paragenetic sequence. Analyzing and understanding the sequence of their chronological sequence of fracture systems, their characteristics, and their distribution will provide insight into the migration and accumulation of hydrocarbons within the geological framework. Therefore, understanding the fracture systems is essential and can significantly impact reservoir quality by facilitating fluid flow and influencing the mechanical behavior of source rocks during hydrocarbon generation and migration processes.

This study will involve a detailed evaluation of the various types of fractures, including their cementation and paragenetic sequence, as well as petrographic observation of the different phases of dolomite formation and stylolitization, LAS, and HAS, to study the characteristics of petrography and paragenesis under various settings. Thus, the sequence of various cement formation associated with the fracture stages, and providing insights into the diagenetic history of the source rocks as well, will be provided in this study.

3. Geological setting

The Upper Jurassic Barsarin Formation occurs in the High Folded, Imbricated, and northern Thrust Zones of Iraq (Fig. 1), and probably continues in the same structural zones towards Turkey and Iran (Buday, 1980). Resulting from the tectonic activity of the Arabian plate and the development of the southern Neo-Tethys ocean (Jassim and Goff, 2006). This ocean had sea level variations that influenced evaporitic sabkhas in the basin during the Jurassic-Cretaceous period (Salih et al., 2021). NE Iraq established an euxinic basin isolated from the Neo-Tethys by a rifted basin where shallow-water carbonates occurred (Jassim and Goff, 2006). The type locality and type section of the Barsarin Formation are situated in the Balambo-Tanjero zone in Barsarin village, northeast of the Rowanduz district in Iraq. Buday (1980) examined the contacts of the Barsarin Formation in the type locality; they seem to be conformable; nonetheless, the base of this formation in the northern thrust zone was characterized by the presence of ferruginous and detrital strata. The initial occurrence of stromatolites signifies the beginning of the Barsarin Formation as observed at the outcrop (Salae, 2001).

The formation reported previously as it contains limestones and dolomitic limestones, characterized by lamination, some with a fluffy texture, locally cherty, alternating between normal layers and crumbled, brecciated, and contorted beds Buday (1980), represented by basin-floor evaporite facies (Sadooni, 1997). The brecciated

strata exhibit a combination of marl and shale (Buday, 1980). The dissolution of anhydrite layers is the origin of the breccia formations (Bellen et al., 1959).

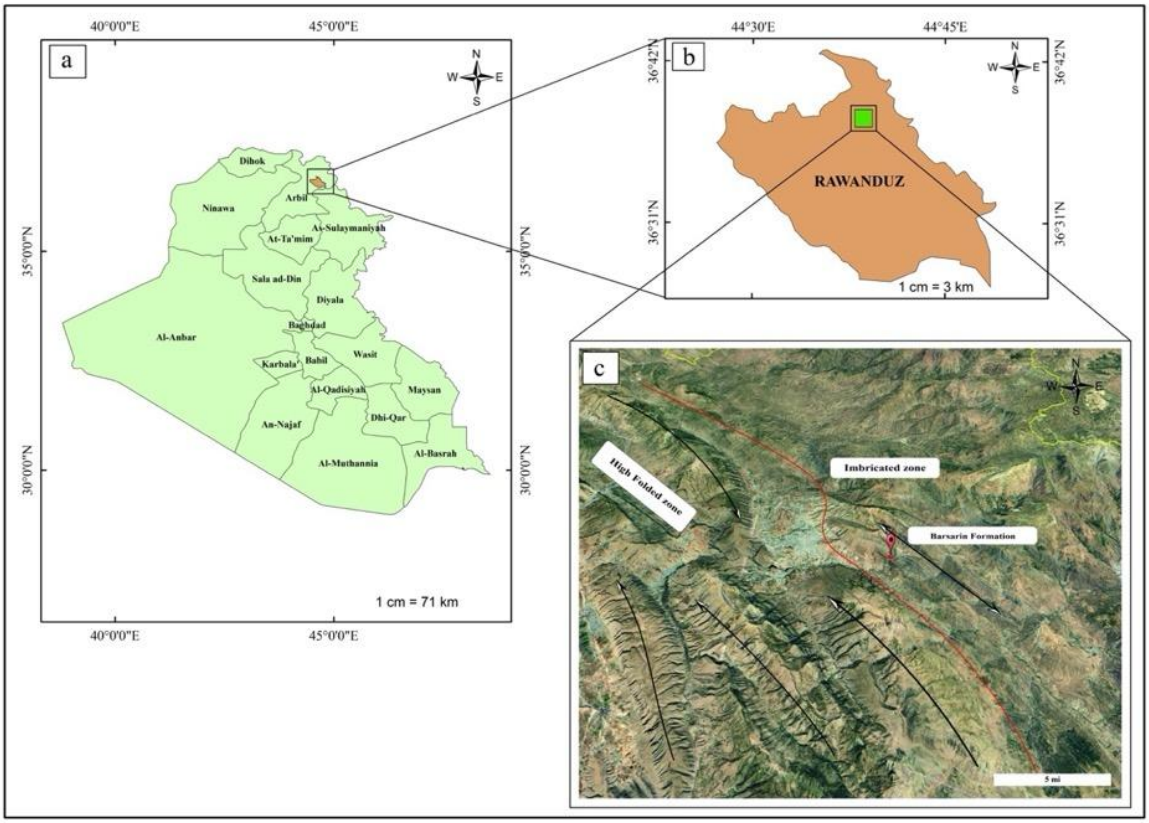

Fig. 1: (a) Simplified general map of Iraq; (b-c) location map and satellite image of the studied area.

4. Materials and Methods

Detailed fieldwork was conducted at the studied section (Fig.1); a total of twenty-seven samples were collected from the outcrop of the Barsarin Formation, specifically from dolomitic and dolomitic limestone at various litho-stratigraphic levels, with sampling predominantly following a NW-SE orientation. Thirty-three samples were prepared for thin-section examination in the laboratory. A slab was initially extracted from each rock sample via a diamond saw to accommodate a microscope slide. After drying on a hot plate, the lapped face of the slab was bonded to a glass slide using epoxy resin. The slab was sectioned with a thin-section saw, with cuts made close to the slide, and further reduced on a thin-section grinder. The section was subsequently final lapped using 600-grit carborundum on a glass plate, with an optional fine grinding phase employing 1000-grit carborundum before polishing. Polishing was conducted on a nylon cloth using diamond paste and a polishing equipment to attain a surface appropriate for meticulous microscopic analysis. The produced thin sections were subsequently examined using a LEICA DM2700P polarized optical microscope, concentrating on the identification of various carbonate phases, the geometric correlations of fractures and veins, and the analysis of cementation types and origins (Fig. 2).

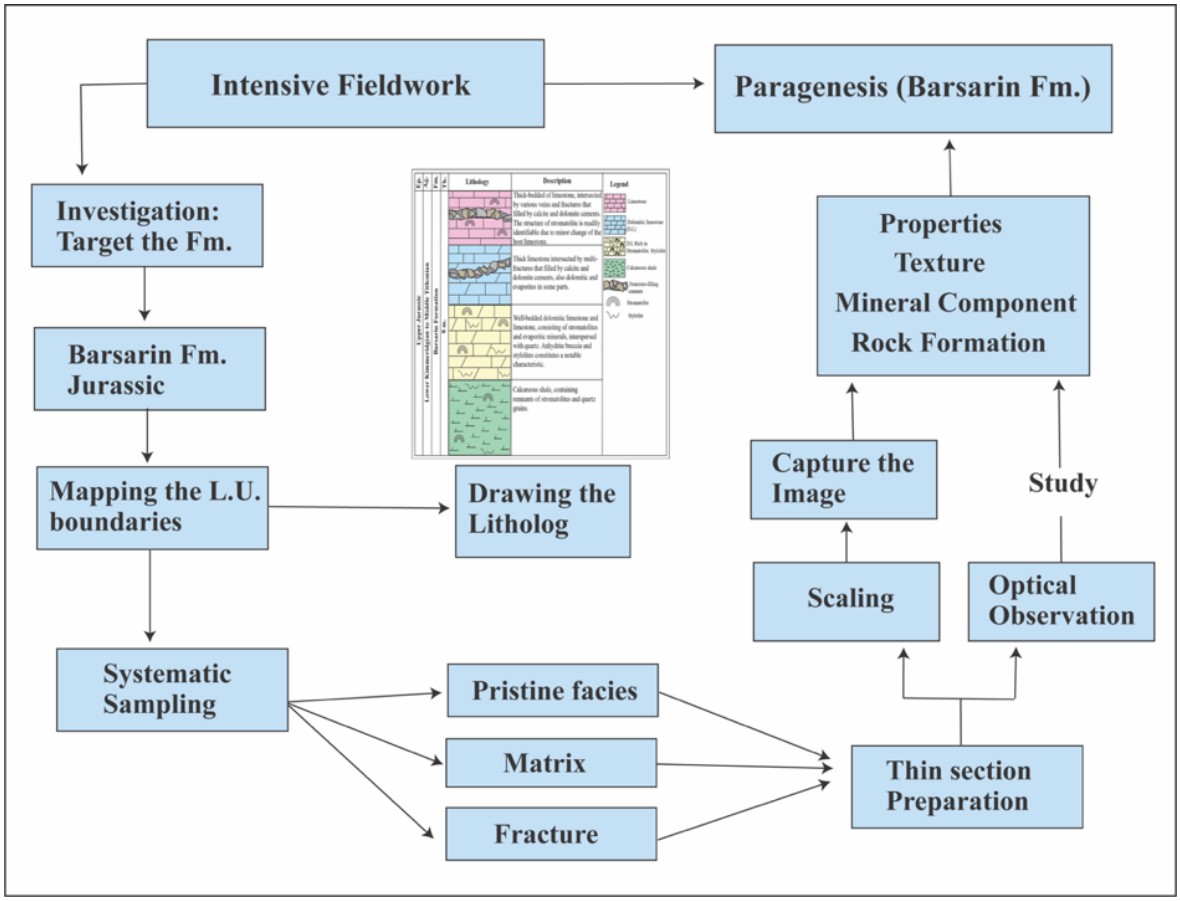

Fig. 2: Flow diagram illustrating the process of the work plan starting from fieldwork to the final stage of paragenesis of the Barbarian Formation.

5. Results and Discussions

A. Field observation

The lower part of the Barsarin Formation consists of decimeter-thick layers less than 30 centimeters with stromatolites and evaporites. Alternation of well-bedded dolomitic and shaly limestones is well recognized in the field. The upper part of the formation consists of distinctive limestones and dolomitic limestones. The thickness of the succession in the examined section type is around 8 meters. Fossils are absent in surface and subsurface rocks due to extensive dolomitization and recrystallisation. The formation has been dated to the Kimmeridgian-Early Tithonian using stratigraphic position, with the underlying Late Tithonian Chia Gara Formation and overlying Kimmeridgian-Oxfordian Naokelekan Formation (Jassim and Goff, 2006). In the study area, some layers in the upper part show two white and dark grey alternating bands. The dark grey band corresponds to the matrix of the rock, varies from mm to cm in width, while the white band is mostly represented by a fracture-filling cement, ranging from mm to cm in size. These banded layers are usually arranged in parallel and oblique directions corresponding to the bedding plane. Additionally, hard dolomitic rocks filling the fractures are also recognized in the field (Figs. 3 and 4).

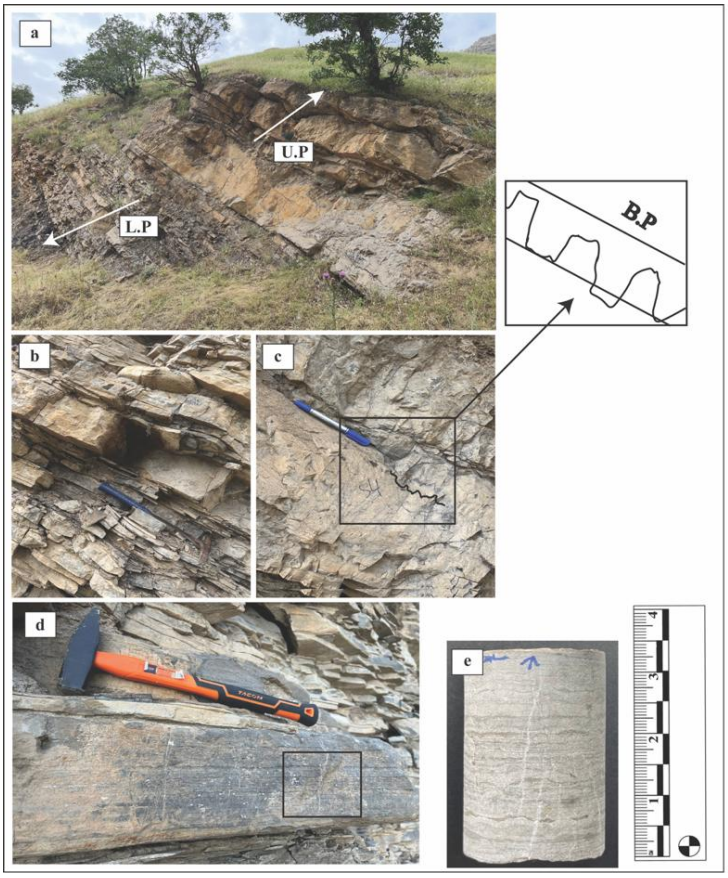

Fig. 3: Field photographs showing the studied section: (a) the lower (L.P) and upper parts (U.P) represented by thin well-bedded and massive layers, respectively (Not to scale), (b) thin-layered rocks, Sample 2. Not to scale. (c) thick-layered rocks, close up the high amplitude stylolite lined in parallel to bedding plane (B.P). Sample 4. (d) thick-layered stromatolite. Sample 10, (e) core sample obtained from a stromatolitic bed. Sample 10.

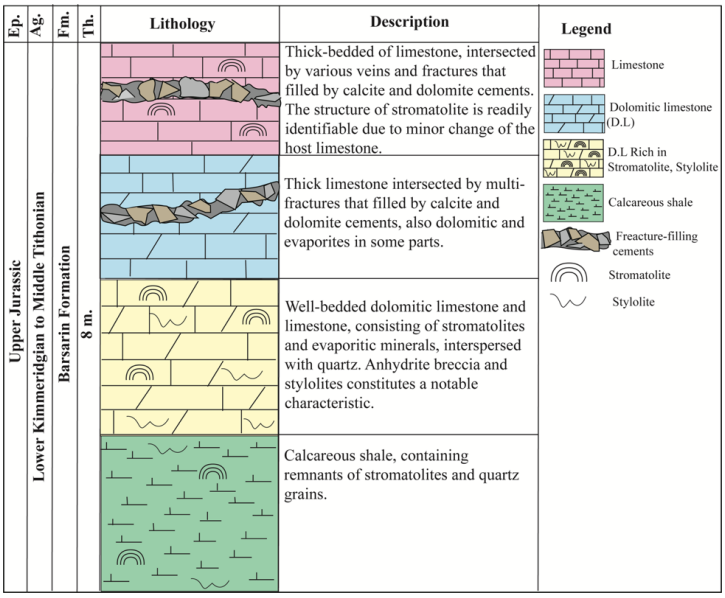

Fig. 4: Litho-log section illustrating the detailed description of the Barsarin Formation in the field.

B. Petrographical Observations

I. non-diagenetic phase "Pristine facies"

a. Stromatolitic boundstone

The main distinctive feature in the depositional facies is the stromatolitic boundstone, considered the original facies of the Barsarin Formation (Fig. 5). In places, stromatolites underwent partial to intensive alteration due to

multi-diagenetic stage processes (Fig. 5a, b). Due to physical compaction, stromatolites suffered textural distortion (Fig. 5c). The sizes of the stromatolites varied from mm- to cm. Sub- to euhedral dolomite crystals are well developed and follow the horizontal laminae of the stromatolite (See Fig. 5d). Associated with this boundstone is a clayey mudstone, with microscopic clay particles (smaller than 0.05mm) that are invisible to the naked eye. These small particles can accumulate in calm, low-energy environments such as lakes, tidal flats, and the deep ocean. The latter facies is partly micritic, with coatings around the grains; the matrix is also microsparitic due to earlier diagenesis. Cyanobacteria are the main organisms that contribute to the formation of microbial mats, previously referred to as 'algal' mats, and are consequently significant in producing laminated carbonate deposits that are called stromatolites (Adams and MacKenzie, 1998). During the depositional environment, these particles comprise organic-rich microbial mats layered with layers of sediment that have precipitated or been deposited on the mat surface (Adams and MacKenzie, 1998). Stromatolites are present throughout the geological record, but they are considered a significant fossil in the Precambrian time because they are utilized for stratigraphic correlation (Tucker, 1981). The most basic kinds of stromatolites, known as "stromatolitic boundstone," are typically located in confined tidal flat environments (Sardarabadi et al., 2016). The amplitude of stromatolites would increase with burial depth. Flat stromatolites are predominantly found in low-energy situations such as supratidal or upper intertidal zones (Sardarabadi et al., 2016). Flat laminated and low- to high-amplitude stromatolites are the predominant features in the current study. The term stromatolite refers to layered microbial deposits (Riding, 1999). Stromatolitic lamination has the greatest impact on weathered surfaces, exhibiting greater irregularity and less development on steep-sided columns (Riding and Tomas, 2006). The association of bedded dolomite with stromatolite structures would probably be indicative of the supratidal and intertidal environments. To support this origin, the evaporite minerals are dominant in the early diagenetic stage. The same case has been documented in various sedimentary structures that can be considered as the direct key for the environmental conditions in the supratidal and intertidal environments in which evaporation would likely occur, and evaporation and stromatolite are associated with bedded dolomites (Prothero and Schwab, 2004).

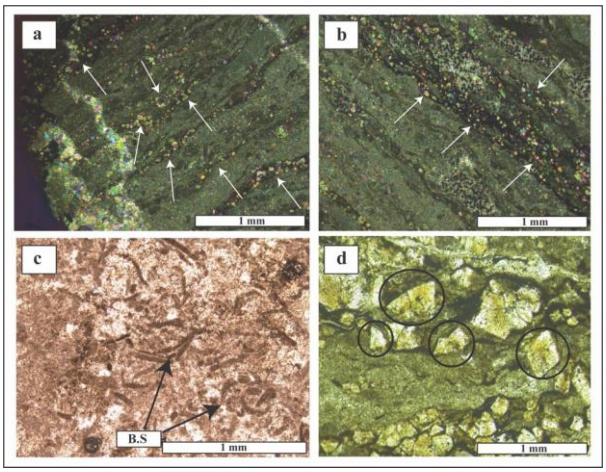

Fig. 5: Photomicrographs show the compaction detected in the thin sections (a, b) the white arrows shows that the stromatolite undergone extensive dolomitization, close up the dolomite grains that arranged in-line with stromatolite distribution, suggesting that stromatolite and dolomite formed at the same time, sample (J1), (c) black arrows show the floating and breaking fragments of stromatolite (B.S) into different pieces due to increasing of compaction associated with stress, sample (J2). (d) black circles show the rhombohedral to subhedral dolomitic crystals, sample (J3).

b. Fenestrae pore-space and Microspar

These two features are considered to be earlier alteration in the studied section, or shortly after deposition. Fenestrae are pore spaces that exceed the typical size of grain-supported voids; they originate from a combination of desiccation and the entrapment of gas bubbles inside the sediment (Adams and MacKenzie, 1998). Fenestral porosity predominantly arises in

carbonate mud-rich sediments of tidal flats, frequently linked to the decomposition of organic matter from cyanobacterial mats (Adams and MacKenzie, 1998). Porosity in carbonate rocks is essential for understanding diagenetic processes and highly significant in evaluating the reservoir rocks. Fenestral porosity in carbonate rocks is fabric selective (Fig. 6a). Fenestral porosity will not constitute effective reservoir rocks unless the fenestrae are interconnected to provide adequate permeability.

Furthermore, microspar is recognized by fine, crystalline calcite comprising crystals from 4–10µm, produced through the recrystallisation of micrite (Bourouni et al., 2017). These fine-grained crystals produced micropore intercrystalline networks filled by hydrocarbons and probably could be associated with fine-grained dolomitization. Accumulation of hydrocarbons in pore space and in-between microspar has also been recognized under an optical microscope (Fig. 6b).

c. Silicification

Silicification is the process where the original skeletal material is replaced by the simultaneous dissolution of calcium carbonate and the precipitation of silica (Butts, 2014). The processes may be facilitated by the nucleation of silica onto organic matter surrounding the mineral crystallites, for example within a shell Butts (2014), or may occur during early or late diagenesis "silicification". The process involves the selective replacement of fossils or the formation of chert layers and nodules, as shown in the Barsarin Formation (Salih et al., 2021). Siliceous skeletal grains, providing a silica supply, comprise sponge spicules in shelf environmental conditions, as well as diatoms and radiolarians in deeper seas. The silicification phase is one of the prominent features in most of the marine facies and diagenetic fluids (Fig. 6c, d). The abundant growth of pyramidal quartz crystals highlights a 'pervasive' silicification and crosscuts the bioclasts and the stylolites or pressure solution joints, as also observed under an optical microscope.

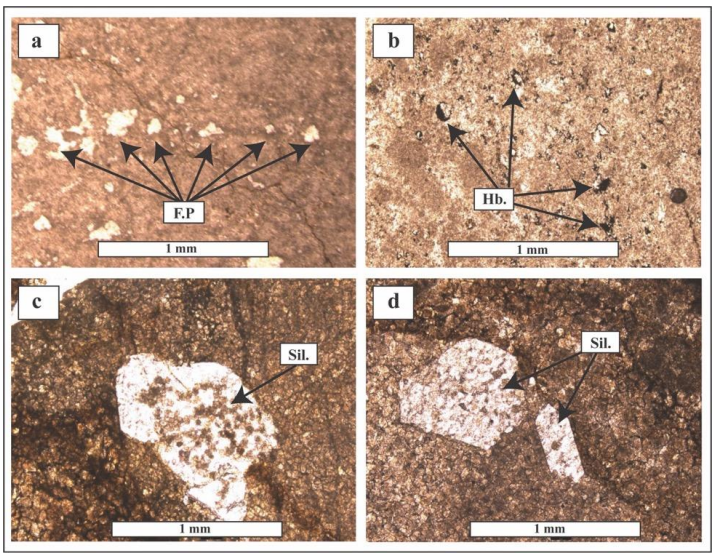

Fig. 6: (PPL) photomicrographs showing (a) Fenestral porosity, sample (J4), (b) micropore filled by hydrocarbon (Hb) also hydrocarbon (Hb) between microsparitoc- pore space, sample (J5), (c-d) silicification (Sil.), samples (J6 and J7).

II. Diagenetic Phase-early, near-surface, and late deep-burial diagenesis

Six different types of dolomites were recognized based on their characteristics and physical properties under two different environmental settings:

a. Dolomite Brecciation (DB) and anhedral-subhedral dolomite (DA)

In situ brecciation of dolomites and floating of dolomite grains within anhydrite bodies (leaching of anhydrite) is a distinctive feature of early diagenesis (Salih et al., 2021). This kind of feature is similar to brecciated texture (Fig. 7a). Anhydrite cements offer the clearest indication of the date of matrix dolomitization in relation to early diagenesis (Adams and Diamond, 2017). Anhydrite cementation is a prevalent characteristic that may be linked to seepage reflux dolomites (Ruppel and Cander, 1988; Rahimpour-Bonab et al., 2010). Calcium ions released during dolomitization interact with sulfate-rich refluxing

brines Machel (2004), and the region of maximum anhydrite cementation typically coincides with the dolomitization process. This area is unstable and susceptible to alteration by following fluids (Jones and Xiao, 2005; Al-Helal et al., 2012).

The anhedral-subhedral dolomite (D_A) is characterized by sub-planar crystals, tightly packed crystals, with persisting micrite products that predate this phase "D_A", and the crystals commonly have a unit extinction under cross-nicols. Therefore, both dolomite phases probably could be linked to early diagenesis and near-surface conditions since the collapse of mimic dolomite still preserved the pristine facies (Fig. 7b).

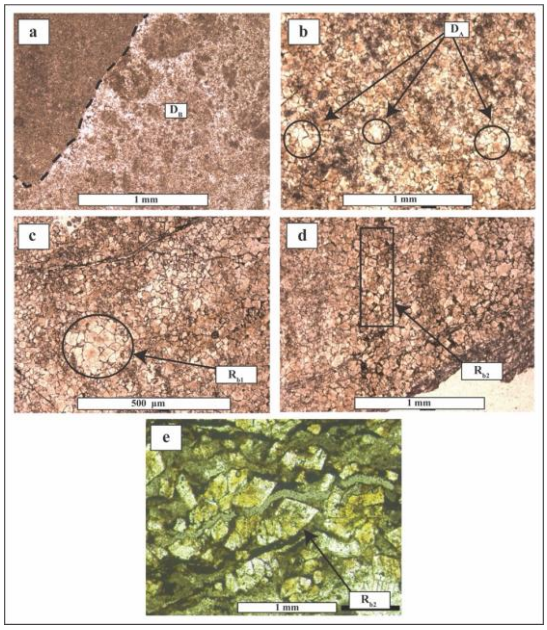

Fig. 7: Photomicrographs illustrating (a) brecciation of dolomite; D_B shows a dolomite brecciation in close contact with micrite facies, sample (J8). The area above the dotted line represents the early paragenetic sequence and predates D_B; (b) show the aggregation of dolomite from anhedral, small-sized dolomite to subhedral large size dolomite crystals (see black circles), (J9), (c-e) dolomitization phases, Samples: (J10, J10, J11). (c) The black circle shows semi-rhombohedral dolomite (Rb_1), Sample (J10). (d) The black rectangle shows rhombohedral dolomite (Rb_2), Sample (J10). (e) The black arrow shows rhombohedral dolomite (Rb_2), Sample (J11).

b. Semi-Rhombohedral Dolomites (Rb1)

This type of dolomite is characterized by semi-rhombohedral crystals (5µm-110µm) and completely rhombohedral crystals (Fig. 7c) within a tight textural appearance. The dolomite crystals show a partial preservation of pristine facies (micrite preservation), suggesting an early replacement process (Elias Bahnan et al., 2021). Fine crystalline dolomite (Rb_1) is related to one of the initial stages of dolomitization that impacted the mudstone facies. Rb_1 could also be linked to stylolite formation as it coincides with early stylolitization. The origin of Mg-rich fluids suggests that Rb_1 may have originated as a result of evaporation; the same case has been reported by Zhang et al. (2022). Fine-crystalline dolomite microcrystals (Rb_1) typically exhibit sub-planar rhombic textures, signifying that Rb_1 formed at comparatively low temperatures during the first shallow burial phase (Sibley and Gregg, 1987).

c. Rhombohedral Dolomite (Rb_2)

Rb_2 dolomite consists of coarse crystalline, planar euhedral dolomite, in places with a distinct zonation with a clear rim and cloudy core (Fig. 7d, e). The rim of crystals is clear, displaying a white color indicating a higher replacement exchange. Rb_2 substitutes for Rb_1 in the most permeable regions, yielding non-mimetic, medium to coarse planar euhedral crystal mosaics, and characterized by high porosity and permeability compared to Rb_1 dolomite. The primary distinctions between these two phases of dolomites in the literature are based on the increased crystal size and the occurrence of zonation within late dolomitic crystals (Gomez-Rivas et al., 2022). This suggests that rhombohedral dolomite cements were found under higher temperatures than those of semi-rhombohedral dolomite (Gregg and Sibley, 1984, Gregg and Shelton, 1990). Rd_2 dolomites have larger crystal sizes compared to Rd_1 and display an interconnected mosaic of planar to anhedral shapes.

d. Radiaxial calcite-filling fractures (R_X)

Radiaxial cement (R_X) consists of large, elongate calcite crystals, forming a single phase in a multi-fracturing system. Fracture-filling R_X cement has two sets of cleavages arranged at an acute angle (Fig. 8a, b). These cleavages show a curved surface, which usually might give a sweepy extinction, and twin planes under crossed nicols. In the literature, radiaxial cements have been represented by fibrous calcite cement and considered as a marine or replacement cement (Kim and Lee, 2003). Radiaxial cements are widespread pore-filling cements in ancient limestones, characterized by a unique combination of curved twins, convergent optic axes, and divergent sub-crystals inside a singular crystal (Davies, 1977; Saller, 1986). Other scholars added

that radiaxial fibrous calcite is a substitution for fibrous aragonite or high-Mg calcite (Bathurst, 1972; Kendall and Tucker, 1973), that it can form through the precipitation of low-Mg and high-Mg calcite, and that crystal development is asymmetric (James and Jones, 2015). High-Mg calcite types might be replaced by low-Mg calcite during burial. Primary pores and subsequent fractures are typically bordered with turbid crystals of radiaxial fibrous calcite (Kendall, 1985). Radiaxial fibrous calcite typically constitutes the initial production of pore-lining cement, and radiaxial fibrous calcite is viewed as the original calcite cement that formed during shallow burial in marine pore fluids (Bishop et al., 2014). However, the radiaxial dolomite cement in our study requires different environmental conditions than those previously documented in the literature. The twisted cleavage of R_X and the associated stylolitic features with R_X cement, and sweepy extinction of these crystals under crossed nicols definitely require higher temperature conditions than those reported previously. Therefore, paragenetically, the radiaxial calcite-filling fractures predate saddle dolomite formation.

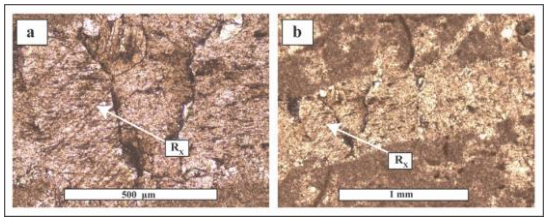

Fig. 8: (PPL) photomicrographs (a-b) white arrows show a single crystal of radiaxial cement inside the fracture, Sample (J12).

e. Saddle Dolomite (SD)

Saddle dolomites have larger crystal sizes (up to 650µm) than those of D_B, D_A, Rb_1, and Rb_2, and develop a typical curved habit with a sweepy extinction. All these properties indicate that SD may have developed from the fast precipitation of high temperatures with magnesium-rich fluids during diagenesis. The same case has been reported by (Machel, 2004, Davies and Smith Jr, 2006). The homogenization temperature from microthermometry analyses and fluid inclusions suggests that SD can originate from hydrothermal fluids, higher than >200°C (Zhang et al., 2022). A large number of saddle dolomite assemblages consist of anhedral crystals in mosaic aggregates with uneven borders (Yu et al., 2019). However, the literature does not give information about the petrographic composition between burial hydrothermal dolomitization (BHD) and shallow hydrothermal dolomitization (SHD). The primary characteristics of BHD are the corrosion boundaries between the attached grains, which could be linked to high pressure or the compaction process during burial. Furthermore, the dissolution process occurred later during burial diagenesis, likely at depths over 2km inside the late burial diagenesis of SD-filling fractures. Dissolution of carbonates, or burial corrosion, is a predominant phenomenon in the subsurface that frequently develops near transtensional active faults and serves as channels for hydrothermal fluids that evolve, potentially resulting in various forms of mineralization and dissolution (Smith, 2013). Furthermore, the zigzag boundaries between the SD grains, "suture contacts," are another indicator of BHD (Fig. 9a-f).

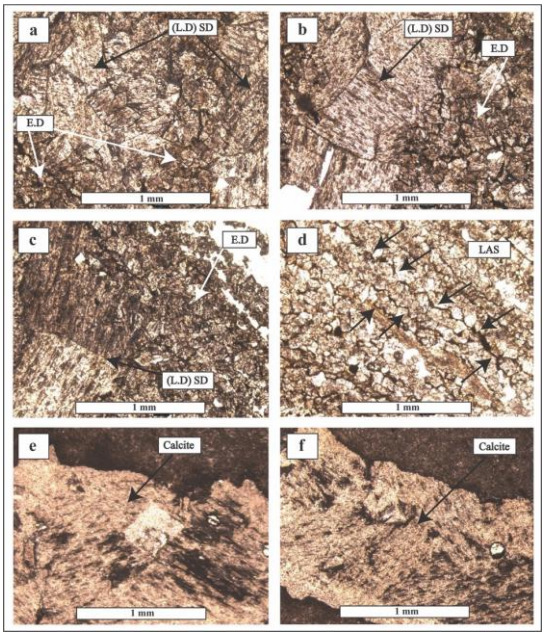

Fig. 9: Photomicrographs of BHD within saddle dolomites illustrating: (a - c) black arrows show Late Dolomitization (L.D.) coarse crystals of saddle dolomite (SD. White arrows show Early Dolomitization (E.D), fine-sized crystals of saddle dolomite. (d) LAS Low Amplitude Stylolization, sample (J13). (e,f) black arrows show calcite formation filling the fracture, sample (J14).

III Mechanical stylolitization controlled by increasing burial depth

Stylolitization provides preferential pathways for large-scale fluid flow, resulting in spatial and temporal variations of reservoir heterogeneities in

carbonate successions (Morad et al., 2018). During the diagenetic features of carbonate rocks and the tectonic compression phase in foreland basins, stylolites are considered conduits for the flow of hydrocarbons and hot basinal brines (Paganoni et al., 2016). These brines can lead to the precipitation of minerals such as saddle dolomite, calcite, fluorite, and sphalerite, characteristic of hydrothermal ore deposits, adjacent to and within the proximity of stylolites (Vandeginste and John, 2013; Mansurbeg et al., 2016). They are believed to arise from pressure-induced dissolution caused by overburden stress or tectonic compression (Ameen et al., 2010). The function of stylolites is as conduits as well as obstructions for fluid movement (Baron and Parnell, 2007; Heap et al., 2014). Some scholars have reported that the dissolution of limestone along the stylolite may provide dolomitization through the movement of Mg-rich fluids or hydrocarbons (Tondi et al., 2006; Merino and Canals, 2011). Consequently, fine-crystalline dolomite cements linked to stylolite may occur concurrently with or after stylolite development (Dunnington, 1954). Stylolite was generated through chemical compression and exhibits varied scales and dimensions. Certain researchers have reported that pressure dissolution appeared at depths of 610 to 914 meters, forming stylolites (Dunnington, 1954), which can potentially be observed in a profound burial environment (Tang, 2007). Over the past few years, researchers have suggested that stylolites develop at depths ranging from 500 meters to 1 kilometer (Beaudoin et al., 2016). Different and distinctive types of bedding-parallel stylolites were identified in the research area, suggesting that the Barsarin Formation experienced varying vertical stress as a result of mechanical compaction and vertical overburden stress.

Two types of stylolites are recognized in the studied area. The low amplitude stylolites (LAS) are associated with microspar and anhedral dolomitization, while the high amplitude stylolites (HAS) are usually associated with radiaxial cement (Fig. 10a, b), burial dolomitization and calcite formation, and postdate the LAS (Fig. 10c, d). Therefore, LAS suggest early subsidence or shallow burial diagenesis of the Barsarin Formation, while HAS strongly favors the continuous increasing of burial depth. The key indicators for increasing the vertical stress due to increasing burial depth are: (i) increase in the distance between the crest and the trough of stylolite (amplitude), (ii) LAS synchronizes with early diagenetic fluids, while HAS synchronizes with late diagenetic fluids, (iii) HAS is associated with a vertical multi-fracturing system parallel to burial depth, while LAS does not coincide with any fracture system, in places crosscut by the early fracturing stage. Furthermore, both stylolites lack any evidence of shearing deformation, and this is an indication that these stylolites formed due to continuous increasing of burial weight of overlying sequence formations.

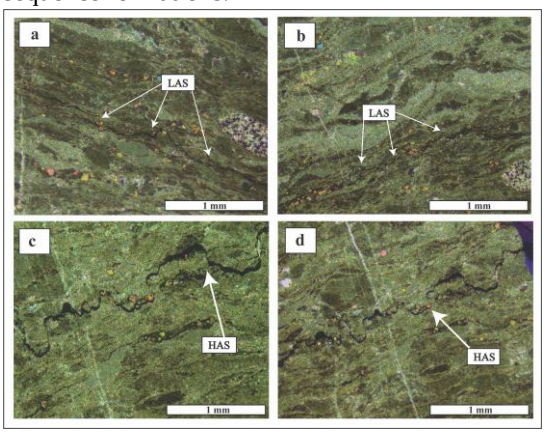

Fig. 10: Photomicrographs (a, b). White arrows show Low-amplitude stylolite (LAS) post-dated Rb_1 fabric. (c, d) white arrows show high-amplitude stylolite (HAS), Sample (J15).

IV Staging of multi-fracture system in Upper Jurassic source rock

In addition to the depositional and early diagenetic facies, the following multi-fracture stages were recognized under an optical microscope:

Fracture I (FI): The earliest fracture formation was identified in the Barsarin Formation, a fracture filled by calcite cement with variable-sized crystals in a mosaic shape (Fig. 11). The FI-filled calcite cement crosscuts the early stylolite. The early stylolites were characterized by a low amplitude pattern (LAS) and usually followed the stromatolitic facies pattern (Fig. 10a-b). However, the late stylolite was characterized by a high amplitude pattern (HAS) developed also within the various matrix facies.

Fracture II (FII): This fracture type is also filled by calcite crystals and post-dates the FI and the initial bedding-parallel stylolite (LAS). The crystal shape was characterized by an anhedral-subhedral crystal shape within a compacted texture.

Fracture III (FIII): This type of fracture is characterized by euhedral to subhedral grains with variable sizes of calcite crystals, usually with the medium-sized crystals formed close to the fracture wall and the size growing toward the fracture core.

Fracture IV (FIV): FIV is the largest fracture filled by elongate shapes of calcite crystals in a complex set of fractures. It is usually filled by radiaxial calcite crystals, likely formed from re-opening of an earlier fracture. The re-opened fracture extends through host limestone/dolomite matrix facies. The re-opening fracture was likely formed under high pressure and deep burial conditions due to the corrosive and dissolution surface of the radiaxial cement and the sweepy/curved shapes of the crystals filling this fracture. The development of suture contact, compacted zigzag shapes between dolomite crystals, and dissolution features support deep burial diagenesis.

Fracture V (FV): This fracture is associated with saddle dolomite formation and contains disturbed solid bitumen inclusions, likely hydrocarbon inclusions (Fig. 12). Suture contact between previous dolomitization and fracture-filled saddle dolomite, corrosion, and compacting of SD crystals are likely linked to increasing subsidence rate and overlying sedimentary rocks. The diagenetic setting of the last phase of dolomitization is similar to that of the deep diagenetic "Mesogenesis Phase". Saddle dolomite formation and its mechanism can be recognized by their appearance and features under deep conditions.

Burial corrosion is a form of selective dissolution that occurs in the burial diagenetic environment, characterized by significant selective dissolution following cementation and pressure solution, with distinguished zigzag wall of dolomite crystals that is consistent with stylolite occurrence. Stylolites that separate two dolomites function as conduits for fluids or hydrocarbons. It is most likely formed under high pressure/temperature because the crystals of dolomite have a sweepy texture that gives a curved shape. There are two different cement formations, formed by two different fluid sources, suggesting a spanning of cementation time intervals.

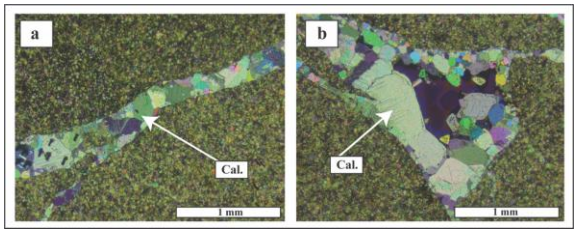

Fig. 11: Microphotographs. (a, b) illustrating fracture-filling calcite cement (FI), Cal. = calcite, Sample (J16).

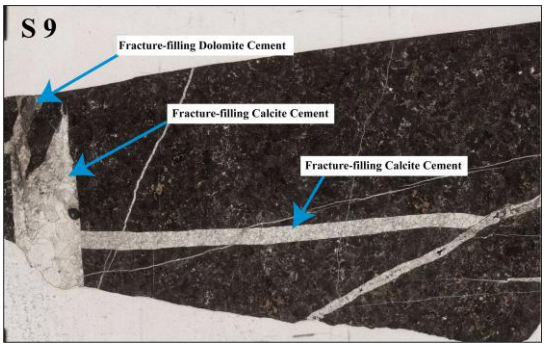

Fig. 12: Image scanning of thin section showing multi-fractures that are filled by various types of cements, sample (J17).

V Timing of fracturing and diagenetic fluids

Fractures can be categorized as structural and dissolution fractures based on their origin (Yang et al., 2004; Zhao et al., 2012). The deformation stress facilitates the development of structural fractures, encompassing low-angle, oblique, and high-angle fractures (Zhang et al., 2022). Since the diagenetic fluids have primarily dissolved the structural fractures or unstable rocks, curved and smooth fracture edges will be produced (Salih et al., 2023; Salih, 2023). Hydrothermal minerals and black residual bitumen in the dissolution fractures suggest that the dissolution fluid may be either hydrothermal or organic acid fluid (Salih et al., 2019a, b). The extent of fill is influenced by the fracture size (a smaller volume relative to surface area facilitates the sealing of narrower fractures, assuming other factors remain constant) and the rate at which the fracture opened (Lander and Laubach, 2014). Thermal exposure, geochemical conditions, and the reactivity and composition of the fracture wall rocks could be involved in the length and size of fracture opening. One facet of fracture diagenesis is the ability of the host rock to supply reactants through localized dissolution and diffusion (Gale et al., 2014). Certain fractures exhibit planes with many host-rock inclusions aligned parallel to the fracture wall, resulting from the crack-seal mechanism during fracture propagation. Some cracks comprise multiple

minerals (Gale et al., 2014). The series of fractures can be categorized based on the intersecting and geometrical relationships. In the early stage of fracturing, the low-angle and oblique fractures predominantly developed and were subsequently filled with calcite cements. In the final stages, high-angle, re-opening, subsequent, and vertical fractures developed, subsequently filled with medium- to coarse-crystalline calcite and saddle dolomite (SD). Several scholars classified and identified the timing of fractures utilizing various methods or based on various parameters, like cross-cutting of fractures, U-Pb direct dating, fluid inclusion and microthermometry, etc. (Zhang et al., 2022). In addition to using the cross-cutting relationship and geometrical distribution of natural fractures, our study adds a type of fracture-filled cementation that required enough time for the dissolution-cementation/replacement process. Some natural fractures that developed under moderate to profound burial conditions throughout geological time scales are lined or sealed with mineral cement (Laubach, 2003). White-colored, coarse crystalline calcite cement is found in the fracture (FIII). This type of fracture was also associated with a complex set of fractures and was parallel to the amplitude of late stylolites. These fractures probably coincided with the formation of the stylolitization process. The fractures terminated at the wider end of the stylolite, called tension gash. These tension gashes support the mechanical overburden stress due to further increase of burial depth and vertical stress during this stage (Salih et al., 2020).

6. Conclusion

The detailed data and analysis presented in this study provide valuable insights into the generation and evolution of the fracture systems and fluid evolution in shallow and subsurface environmental conditions within the Upper Jurassic Barsarin Formation. The results contribute significantly to the understanding of critical geological processes, petroleum formation, and petroleum applications. Through systematic investigation, five main types of fractures (FI, FII, FIII, FIV, and FV) are recognized. The fracture-filled cements show a distinct characteristic based on their formation conditions, age dynamics, and paragenetic sequence. The identification of these fractures provides a paragenetic sequence of various fracturing stages for future developments in exploration for hydrocarbon source rock and reservoirs. The paragenesis for the different stages of fracture is recognized as follows:

1. FI fractures: formed at surface or near-surface conditions, having an age no older than early stylolite formation (LAS).
2. FII fractures: developed during burial diagenesis, and coeval with later stages of diagenesis.
3. FIII fractures: in-situ fractures formed under subsurface conditions, coinciding with high-amplitude stylolitization.
4. FIV fractures: filled by calcite cement with abundant solid bitumen fluid inclusions, reflecting the increasing burial weight of overlying sedimentary rocks during the "mesogenesis phase."
5. FV-filled dolomite cement, and in places associated with calcite cement.

The FIII and FIV fractures cover a large volume among the other types of fractures, and show a complex history of fracture formation under different re-opening systems, with targeted features and textures indicating a deep burial influence on calcite-cement formation. Fracture V coincides with saddle dolomite formation that is characterized by distinct hydrocarbon inclusions under hot diagenetic conditions. The evolution of the geo-chronological stages of these fractures reveals a significant interaction between fluid movement and pristine facies, particularly under varying pressure and thermal regimes during shallow/deep burial conditions. The distinctions between shallow/deep settings provide a valuable framework for understanding similar geological formations and their respective hydrocarbon potentials.

The findings obtained from this study not only enrich the geological understanding of the Barsarin Formation but also add a new insight into future exploration of similar fractured reservoirs. The recognition of these diagenetic and textural features emphasizes the need for further studies that examine the implications for hydrocarbon accumulation, fluid movement, and sedimentary basin evolution. In brief, such detailed and enhanced studies may lead to more efficient exploration and extraction strategies in the future of natural resources.

7. Future Recommendation

Given the significant implications of the findings from this study, several ways for future research and exploration can be recommended:

1. Utilizing advanced Laser Ablation U-Pb dating using ICP-MS for obtaining absolute, meaningful ages and direct dating of the fracture system within the Barsarin Formation.
2. Future studies could benefit from the integration of advanced imaging technologies such as micro-CT scanning (Computed Tomography) to provide a 3D view of fracture geometries and connectivity within subsurface environments. Such approaches could enhance the accuracy of fracture network models and improve predictions for fluid flow behavior.
3. Detailed petrophysical and geochemical analyses (major, minor, and trace elemental analyses; REE; mineralogical components) could provide the specific processes that governed their formation and how these processes vary across different geological settings.
4. Using a sophisticated technique to determine the paleo-temperature and paleo-pressure of any trapped fluids with each stage of fracture type by utilizing fluid inclusion and microthermometry.
5. Future research should focus on evaluating the environmental impact of utilizing geological formations for reservoir storage, ensuring that methods used align with sustainability aspects.

8. Conflict of Interest

The authors declare that they have no known competing financial interests or personal relationships that could have appeared to influence the recent work.

9. Funding Statement

This research received no external funding.

10. References

Adams, A. and Diamond, L. W. 2017. Early diagenesis driven by widespread meteoric infiltration of a Central European carbonate ramp: A reinterpretation of the Upper Muschelkalk. Sedimentary Geology, 362, 37-52.

Adams, A. and MacKenzie, W. S. 1998. Carbonate sediments and rocks under the microscope: A Colour Atlas, CRC Press, 184 P.

Al-Helal, A. B., Whitaker, F. F. and Xiao, Y. 2012. Reactive transport modeling of brine reflux: dolomitization, anhydrite precipitation, and porosity evolution. Journal of Sedimentary Research, 82, 196-215.

Ameen, M. S., Buhidma, I. M. and Rahim, Z. 2010. The function of fractures and in-situ stresses in the Khuff reservoir performance, onshore fields, Saudi Arabia. AAPG Bulletin, 94, 27-60.

Amirjan, M. and Bozorg, M. 2018. Properties and corrosion behavior of Al based nanocomposite foams produced by the sintering-dissolution process. International Journal of Minerals, Metallurgy, and Materials, 25, 94-101.

André, L., Azaroual, M. and Menjoz, A. 2010. Numerical simulations of the thermal impact of supercritical CO2 injection on chemical reactivity in a carbonate saline reservoir. Transport in porous media, 82, 247-274.

Baqués, V., Ukar, E., Laubach, S. E., Forstner, S. R. and Fall, A. 2020. Fracture, Dissolution, and Cementation Events in Ordovician Carbonate Reservoirs, Tarim Basin, NW China. Geofluids, 2020, 9037429.

Baron, M. and Parnell, J. 2007. Relationships between stylolites and cementation in sandstone reservoirs: Examples from the North Sea, UK and East Greenland. Sedimentary Geology, 194, 17-35.

Bathurst, R. G. 1972. Carbonate sediments and their diagenesis. Elsevier. 1-658 p.

Beaudoin, N., Koehn, D., Lacombe, O., Lecouty, A., Billi, A., Aharonov, E. and Parlangeau, C. 2016. Fingerprinting stress: Stylolite and calcite twinning paleopiezometry revealing the complexity of progressive stress patterns during folding—The case of the Monte Nero anticline in the Apennines, Italy. Tectonics, 35, 1687-1712.

Bellen, R. C., Dunnington, H. V., Wetzel, R. and Morton, D. 1959. Lexique stratigraphique international: Asie. Iraq. Vol. 3C, Centre national de la recherche scientifique. 330 P.

Berra, F. and Carminati, E. 2012. Differential compaction and early rock fracturing in high-relief carbonate platforms: numerical modelling of a Triassic case study (Esino Limestone, Central Southern Alps, Italy). Basin Research, 24, 598-614.

Bishop, J., Montañez, I. and Dy, S. 2014. Meteoric diagenesis and fluid-rock interaction in the Middle Permian Capitan backreef: Yates Formation, Slaughter Canyon, New Mexico. American Association of Petroleum Geology, 98, 1495–1519.

Bjørlykke, K. and Jahren, J. 2012. Open or closed geochemical systems during diagenesis in sedimentary basins: Constraints on mass transfer during diagenesis and the prediction of porosity in sandstone and carbonate reservoirs. AAPG Bulletin, 96, 2193-2214.

Boggs, S. 2006. Principles of Sedimentology and Stratigraphy, Pearson Prentice Hall, 662 P.

Bourouni, P., Tsikouras, B. and Hatzipanagiotou, K. 2017. Petrological investigation of carbonate rocks from the Ionian zone (Etoloakarnania, western Greece). Bulletin of the Geological Society of Greece, 43, 2540.

Buday, T. 1980. The Regional Geology of Iraq, Vol 1: Stratigraphy and Paleogeography. Publications of Geological Survey of Iraq, Baghdad, 445 p.

Budd, D. A., Frost III, E. L., Huntington, K. W. and Allwardt, P. F. 2013. Syndepositional deformation features in high-relief carbonate platforms: long-lived conduits for diagenetic fluids. Journal of Sedimentary Research, 83, 12-36.

Butts, S. H. 2014. Silicification. The Paleontological Society Papers, 20, 15-34.

Davies, G. R. 1977. Former magnesian calcite and aragonite submarine cements in upper Paleozoic reefs of the Canadian Arctic: A summary. Geology, 5, 11-15.

Davies, G. R. and Smith Jr., L. B. 2006. Structurally controlled hydrothermal dolomite reservoir facies: An overview. AAPG Bulletin, 90, 1641-1690.

Dunnington, H. V. 1954. Stylolite development post-dates rock induration. Journal of Sedimentary Research, 24, 27-49.

Elias Bahnan, A., Pironon, J., Carpentier, C., Barré, G. and Gaucher, E. C. 2021. The diagenetic history of the giant Lacq gas field, witness to the Aptian- Albian rifting and the Pyrenean orogeny, revealed by fluid and basin modeling. Marine and Petroleum Geology, 133, 105250.

Fischer, M. P., Higuera-Díaz, I. C., Evans, M. A., Perry, E. C. and Lefticariu, L. 2009. Fracture-controlled paleohydrology in a map-scale detachment fold: Insights from the analysis of fluid inclusions in calcite and quartz veins. Journal of Structural Geology, 31, 1490-1510.

Gale, J. F. W., Laubach, S. E., Marrett, R. A., Olson, J. E., Holder, J. and Reed, R. M. 2004. Predicting and characterizing fractures in dolostone reservoirs: using the link between diagenesis and fracturing. Geological Society, London, Special Publications, 235, 177-192.

Gale, J. F. W., Laubach, S. E., Olson, J. E., Eichhubl, P. and Fall, A. 2014. Natural fractures in shale: A review and new observations. AAPG Bulletin, 98, 2165-2216.

Gomez-Rivas, E., Martín-Martín, J. D., Bons, P. D., Koehn, D., Griera, A., Travé, A., Llorens, M.-G., Humphrey, E. and Neilson, J. 2022. Stylolites and stylolite networks as primary controls on the geometry and distribution of carbonate diagenetic alterations. Marine and Petroleum Geology, 136, 105444.

Gregg, J. M. and Shelton, K. L. 1990. Dolomitization and dolomite neomorphism in the back reef facies of the Bonneterre and Davis formations (Cambrian), southeastern Missouri. Journal of Sedimentary Research, 60, 549-562.

Gregg, J. M. and Sibley, D. F. 1984. Epigenetic dolomitization and the origin of xenotopic dolomite texture. Journal of Sedimentary Research, 54, 908-931.

Heap, M. J., Baud, P., Reuschlé, T. and Meredith, P. G. 2014. Stylolites in limestones: Barriers to fluid flow? Geology, 42, 51-54.

Hooker, J. N. and Katz, R. F. 2015. Vein spacing in extending, layered rock: The effect of synkinematic cementation. American Journal of Science, 315, 557-588.

James, N. P. and Jones, B. 2015. Origin of Carbonate Sedimentary Rocks, John Wiley and Sons, 446 P.

Jassim, S. Z. and Goff, J. C. 2006. Geology of Iraq, DOLIN, SRO, distributed by Geological Society of London.

Jiang, L., Cai, C., Worden, R. H., Crowley, S. F., Jia, L., Zhang, K. and Duncan, I. J. 2016. Multiphase dolomitization of deeply buried Cambrian petroleum reservoirs, Tarim Basin, north-west China. Sedimentology, 63, 2130-2157.

Jiayu, G. 1999. Characteristics and evolutional models of karst reservoirs of lower Ordovician carbonate rocks in the Lunnan area of Tarim Basin. Chinese journal of arid land research, 12, 317-324.

Jones, G. D. and Xiao, Y. 2005. Dolomitization, anhydrite cementation, and porosity evolution in a reflux system: Insights from reactive transport models. AAPG Bulletin, 89, 577-601.

Kendall, A. C. 1985. Radiaxial Fibrous Calcite: A Reappraisal, 59-77. In: Schneidermann, N. and Harris, P. M. (eds.) Carbonate Cements: Based on a Symposium Sponsored by the Society of Economic Paleontologists and Mineralogists. SEPM Society for Sedimentary Geology.

Kendall, A. C. and Tucker, M. E. 1973. Radiaxial fibrous calcite: a replacement after acicular carbonate. Sedimentology, 20, 365-389.

Kim, Y. and Lee, Y. I. 2003. Radiaxial fibrous calcites as low-magnesian calcite cement precipitated in a marine-meteoric mixing zone. Sedimentology, 50, 731-742.

Lander, R. H. and Laubach, S. E. 2014. Insights into rates of fracture growth and sealing from a model for quartz cementation in fractured sandstones. GSA Bulletin, 127, 516-538.

Landry, C. J., Eichhubl, P., Prodanović, M. and Wilkins, S. 2016. Nanoscale grain boundary channels in fracture cement enhance flow in mudrocks. Journal of Geophysical Research: Solid Earth, 121, 3366-3376.

Laubach, S. E. 2003. Practical approaches to identifying sealed and open fractures. AAPG Bulletin, 87, 561-579.

Lee, H. P., Olson, J. E. and Schultz, R. A. 2018. Interaction analysis of propagating opening mode fractures with veins using the Discrete Element Method. International Journal of Rock Mechanics and Mining Sciences, 103, 275-288.

Léveillé, R. J., Bridges, J., Wiens, R. C., Mangold, N., Cousin, A., Lanza, N., Forni, O., Ollila, A., Grotzinger, J. and Clegg, S. 2014. Chemistry of fracture-filling raised ridges in Yellowknife Bay, Gale Crater: Window into past aqueous activity and habitability on Mars.

Journal of Geophysical Research: Planets, 119, 2398-2415.

Lu, Y., Lü, H., Cui, Y. and Chen, H. 2018. Method for fracture effectiveness evaluation based on 3D Mohr Circle and its application. Acta Petrolei Sinica, 39, 564.

Machel, H. G. 2004. Concepts and models of dolomitization: a critical reappraisal. Geological Society, London, Special Publications, 235, 7-63.

Mansurbeg, H., Morad, D., Othman, R., Morad, S., Ceriani, A., Al-Aasm, I., Kolo, K., Spirov, P., Proust, J. N., Preat, A. and Koyi, H. 2016. Hydrothermal dolomitization of the Bekhme formation (Upper Cretaceous), Zagros Basin, Kurdistan Region of Iraq: Record of oil migration and degradation. Sedimentary Geology, 341, 147-162.

McNeill, D. F. and Eberli, G. P. 2009. Early Load-Induced Fracturing in a Prograding Carbonate Margin. Perspectives in carbonate geology: A tribute to the career of Robert Nathan Ginsburg, 327-336.

Merino, E. and Canals, A., 2011. Self-accelerating dolomite-for-calcite replacement: Self-organized dynamics of burial dolomitization and associated mineralization. American Journal of Science, 311, 573 - 607.

Monty, C. L. V. 1976. The origin and development of cryptalgal fabrics. Developments in sedimentology. Elsevier, 193-249.

Morad, D., Nader, F. H., Morad, S., Al Darmaki, F. and Hellevang, H. 2018. Impact of stylolitization on fluid flow and diagenesis in foreland basins: Evidence from an Upper Jurassic carbonate gas reservoir, Abu Dhabi, United Arab Emirates. Journal of Sedimentary Research, 88, 1345-1361.

Oyedokun, O. and Schubert, J. 2017. A quick and energy consistent analytical method for predicting hydraulic fracture propagation through heterogeneous layered media and formations with natural fractures: The use of an effective fracture toughness. Journal of Natural Gas Science and Engineering, 44, 351-364.

Paganoni, M., Al Harthi, A., Morad, D., Morad, S., Ceriani, A., Mansurbeg, H., Al Suwaidi, A., Al-Aasm, I. S., Ehrenberg, S. N. and Sirat, M. 2016. Impact of stylolitization on diagenesis of a Lower Cretaceous carbonate reservoir from a giant oilfield, Abu Dhabi, United Arab Emirates. Sedimentary Geology, 335, 70-92.

Peacock, D. C. P., Nixon, C. W., Rotevatn, A., Sanderson, D. J. and Zuluaga, L. F. 2016. Glossary of fault and other fracture networks. Journal of Structural Geology, 92, 12-29.

Prothero, D. R. and Schwab, F. 2004. Sedimentary geology, Macmillan, 600 P.

Rahimpour-Bonab, H., Esrafili-Dizaji, B. and Tavakoli, V. 2010. Dolomitization and anhydrite precipitation in permo-triassic carbonates at the South Pars gas field, offshore Iran: controls on reservoir quality. Journal of Petroleum Geology, 33, 43-66.

Rasool, R. H., Ali, S. A. and Al-Juboury, A. I. 2023. Petrography and diagenesis of the Middle to Upper Jurassic succession from Sargelu section, northeastern Iraq. Al-Kitab Journal for Pure Sciences, 7, 153-172.

Ren, Q., Jin, Q., Feng, J. and Li, M. 2019. Simulation of stress fields and quantitative prediction of fractures distribution in upper Ordovician biological limestone formation within Hetianhe field, Tarim Basin, NW China. Journal of Petroleum Science and Engineering, 173, 1236-1253.

Riding, R. 1999. The term stromatolite: towards an essential definition. Lethaia, 32, 321-330.

Riding, R. and Tomas, S. 2006. Stromatolite reef crusts, Early Cretaceous, Spain: bacterial origin of in situ-precipitated peloid microspar? Sedimentology, 53, 23-34.

Ruppel, S. C. and Cander, H. S. 1988. Dolomitization of shallow-water platform carbonates by sea water and seawater-derived brines: San Andres Formation (Guadalupian), west Texas in V. Shukla and P. A. Baker, eds., Sedimentology and geochemistry of dolostones: SEPM Special Publication 43, 245–262 P.

Sadooni, F. N. 1997. Stratigraphy and petroleum prospects of Upper Jurassic carbonates in Iraq. Petroleum Geoscience, 3, 233-243.

Salae, A. 2001. Stratigraphy and sedimentology of the Upper Jurassic succession, NE Iraq. University of Baghdad, M Sc thesis, 95 pp.

Salih, N. M. 2023a. The Impact of Hydrothermal Fluids on Porosity Enhancement and Hydrocarbon Migration in Qamchuqa Formation, Lower Cretaceous, Kirkuk Oil Company. Minerals, 13(3), 377. https://doi.org/10.3390/min13030377

Salih, N. M., Al-Majmaie, S. M., and Muhammad, Z. A. 2023. The Porous–Permeable Zones in Heterogeneous Carbonate Reservoirs: A Case Study from Amara Oilfield, Iraq. Proceedings, 87(1), 35. https://doi.org/10.3390/IECG2022-13965

Salih, N., Mansurbeg, H., Kolo, K., Gerdes, A. and Préat, A. 2019a. In situ U-Pb dating of hydrothermal diagenesis in tectonically controlled fracturing in the Upper Cretaceous Bekhme Formation, Kurdistan Region-Iraq. International Geology Review, 62, 2261-2279.

Salih, N., Mansurbeg, H., and Préat, A. 2020. Geochemical and Dynamic Model of Repeated Hydrothermal Injections in Two Mesozoic Successions, Provençal Domain, Maritime Alps, SE-France. Minerals, 10(9), 775. https://doi.org/10.3390/min10090775

Salih, N., Mansurbeg, H., Kolo, K. and Préat, A. 2019b. Hydrothermal carbonate mineralization, calcretization, and microbial diagenesis associated with multiple sedimentary phases in the Upper Cretaceous Bekhme Formation, Kurdistan Region-Iraq. Geosciences, 9, 459.

Salih, N., Préat, A., Gerdes, A., Konhauser, K. and Proust, J.-N. 2021. Tracking the Origin and Evolution of Diagenetic Fluids of Upper Jurassic Carbonate Rocks in the Zagros Thrust Fold Belt, NE-Iraq. Water, 13, 3284.

Saller, A. H. 1986. Radiaxial calcite in lower Miocene strata, subsurface Enewetak Atoll. Journal of Sedimentary Research, 56, 743-762.

Salomon, E., Rotevatn, A., Kristensen, T. B., Grundvåg, S. A., Henstra, G. A., Meckler, A. N., Albert, R. and Gerdes, A. 2020. Fault-controlled fluid circulation and diagenesis along basin-bounding fault systems in rifts – insights from the East Greenland rift system. Solid Earth, 11, 1987-2013.

Sardarabadi, S., Jahani, D. and Ghadimvand, N. 2016. Facies, Depositional Environment and Diagenesis of the Qom Formation in Rameh Section (Northeastern Garmsar). Open Journal of Geology, 6, 1240-1256.

Shen, A., Hu, A., Cheng, T., Liang, F., Pan, W., Feng, Y. and Zhao, J. 2019. Laser ablation in situ U-Pb dating and its application to diagenesis-porosity evolution of carbonate reservoirs. Petroleum Exploration and Development, 46, 1127-1140.

Shen, A., Luo, X., Hu, A., Qiao, Z. and Zhang, J. 2022. Dolomitization evolution and its effects on hydrocarbon reservoir formation from penecontemporaneous to deep burial environment. Petroleum Exploration and Development, 49, 731-743.

Sibley, D. F. and Gregg, J. M. 1987. Classification of dolomite rock textures. Journal of Sedimentary Research, 57, 967-975.

Smith, T. 2013. Subsurface corrosion of calcite dissolution and dolomite by fault-sourced hydrothermal fluids, AAPG Annual Convention and Exhibition, Pittsburgh, Pennsylvania, May 19-22, 2013, Search and Discovery Article #50918.

Sonntag, R., Evans, J. P., Pointe, P. L., Deraps, M., Sisley, H. and Richey, D. 2014. Sedimentological controls on the fracture distribution and network development in Mesaverde Group sandstone lithofacies, Uinta Basin, Utah, USA. Geological Society, London, Special Publications, 374, 23-50.

Tang, J. 2007. The Diagenesis of the Upper Paleozoic Carbonate Rocks in the Southeast Xiang Depression. Journal-Southwest Petroleum Institute, 29, 43.

Tiab, D. and Donaldson, E. 2003. Petrophysics: Theory and Practice of Measuring Reservoir Rock and Fluid Transport Properties: Second Edition, Gulf Professional Publishing - Elsevier, 1008 P.

Tondi, E., Antonellini, M., Aydin, A., Marchegiani, L. and Cello, G. 2006. The role of deformation bands, stylolites and sheared stylolites in fault development in carbonate grainstones of Majella Mountain, Italy. Journal of Structural Geology, 28, 376-391.

Tucker, M. E. 1981. Sedimentary petrology: an introduction. Geoscience Texts. England, 252, 252 P.

Vandeginste, V. and John, C. M. 2013. Diagenetic implications of stylolitization in pelagic carbonates, Canterbury Basin, offshore New Zealand. Journal of Sedimentary Research, 83, 226-240.

Virgo, S., Abe, S. and Urai, J. L. 2014. The evolution of crack seal vein and fracture networks in an evolving stress field: Insights from Discrete Element Models of fracture sealing. Journal of Geophysical Research: Solid Earth, 119, 8708-8727.

Warpinski, N. R. and Lorenz, J. C. 2008. Analysis of the multiwell experiment data and results: Implications for the basin-centered gas model. Vail Hedberg Conference: AAPG Hedberg Series, no. 3, p. 157-176.

Weisenberger, T. B., Eichhubl, P., Laubach, S. E. and Fall, A. 2019. Degradation of fracture porosity in sandstone by carbonate cement, Piceance Basin, Colorado, USA. Petroleum Geoscience, 25, 354-370.

Wennberg, O. P., Casini, G., Jonoud, S. and Peacock, D. C. P. 2016. The characteristics of open fractures in carbonate reservoirs and their impact on fluid flow: a discussion. Petroleum Geoscience, 22, 91-104.

Xu, H., Guo, X., Cao, Z., Alves, T. M., Tao, Z., Wang, B., Chen, J., Zuo, G., Zhang, X. and Luo, T. 2025. Petroleum-charge history of Paleozoic carbonates in the Tahe oil field, Tarim Basin, northwestern China: Insights from oil geochemistry, fluid inclusion, and U-Pb dating. AAPG Bulletin, 109, 57-84.

Xu, J., Zhang, B., Qin, Y., Cao, G. and Zhang, H. 2016. Method for calculating the fracture porosity of tight-fracture reservoirs. GEOPHYSICS, 81, IM57-IM70.

Yang, N., Lü, X. and Pan, W. 2004. Features of fracture development in Ordovician carbonate reservoirs of the Lunnan buried hill. Journal of Xi'an Shiyou University (Natural Science Edition), 19, 40-43.

Yu, K., Qiu, L., Cao, Y., Sun, P., Qu, C. and Yang, Y. 2019. Hydrothermal origin of early Permian saddle dolomites in the Junggar Basin, NW China. Journal of Asian Earth Sciences, 184, 103990.

Zhang, X., Li, Q., You, X., Ma, L., Jing, A., Tian, W. and Wen, L. 2022. Characteristics and formation mechanism of the lower Paleozoic dolomite reservoirs in the Dongying depression, Bohai Bay Basin. Energies, 15, 2155.

Zhao, W., Anjiang, S., Suyun, H., Wenqing, P., JianFeng, Z. and Zhan Feng, Q. 2012. Types and distributional features of Cambrian-Ordovician dolostone reservoirs in Tarim Basin, northwestern China. Acta Petrologica Sinica, 28, 758-768.

Iraqi National Journal of Earth Science, Vol. 26, No. 04, 2026 (01-18)

Iraqi National Journal of Earth Science

www.earth.uomosul.edu.iq

الترتيب ونظام الكسور المتعددة في تكوين البارسارين الجوراسيك: الآثار المترتبة على مواقع الدفن المختلفة، شمال شرق العراق

ريان فتاح [1]، نمام صالح[2*]، الان بريات[3]

rayanmhamadfatah99@gmail.com namam.salih@soran.edu.iq alain.preat@ulb.be

[1] قسم علوم الأرض البترولية، كلية العلوم، جامعة سوران، سوران، أربيل، 44008، العراق.

[2] قسم هندسة البترول والتعدين، كلية الهندسة، جامعة سوران، سوران، أربيل، 44008، العراق.

[3] مجموعة أبحاث الكيمياء الحيوية الجيولوجية ونمذجة نظام الأرض، الجامعة الحرة في بروكسل، 1050، بروكسل، بلجيكا.

* الباحث المراسل.

تاريخ الاستلام: 23 كانون الثاني 2025 تاريخ المراجعة: 20 آذار 2025 تاريخ القبول: 13 أيار 2025

تاريخ النشر الالكتروني: 01 تشرين الأول 2026

الملخص

يلعب تكوّين نظام الكسور وتطور السوائل الجيولوجية في الظروف البيئية الضحلة والعميقة دورًا حاسمًا في مختلف العمليات الجيولوجية وتطبيقات البترول. تُقيّم هذا البحث البيانات الشاملة لتوفير فهم معمق لنظام الكسور المتعددة، الذي تملأه مراحل التماسك/الذوبان المختلفة المرتبطة بسوائل مختلفة قرب السطح وتحته. استخدمت هذه الدراسة مجهرًا ضوئيًا ورصدًا ميدانيًا مكثفًا لتتبع التكوين المستهدف ونظام الكسور اللاحقة في العصر الجوراسيك. حددت الدراسة خمسة أنواع رئيسية من الكسور: (1) FI الناتج عن ظروف سطحية أو قريبة من السطح، حيث بدأت تكوين الكسور ليس أحدث من توقيت ستيلوليت منخفض السعة. (2) الكسور FII المتشكل في دفن ضحل، وكان متزامنًا مع ستيلوليت منخفض السعة "الستيلولايت المبكر". (3) FIII الكسور المتشكل في ظروف تحت سطحية متزامنة مع ستيلوليت عالي السعة(4) الكسور الرابعة (FIV) المملوءة بأسمنت الكالسيت مع وجود كميات وفيرة من شوائب سائل البيتومين الصلب؛ و(5) الكسور الخامسة (FV) المملوءة بأسمنت الدولوميت. ترتبط خصائص ومظهر بلورات الدولوميت، والتآكل، والتلامس الخيطي بين حبيبات الدولوميت السرجي، والحبيبات المضغوطة بإحكام ارتباطًا مباشرًا بزيادة وزن دفن الصخور الرسوبية العلوية "مرحلة التولد المتوسط". باختصار، تُضيف هذه النتائج رؤيةً جديدةً، إذ تُشكّل الكسور قنواتٍ وحواجزَ أساسيةً لهجرة الهيدروكربونات وتراكمها عبر عملياتٍ جيولوجيةٍ مُتنوعة، بدءًا من تكوّنها أثناء الترسيب وصولًا إلى تطورها وأهميتها في بيئات ما بعد الترسيب. ويُمكّن فهم آلية عمل هذه الكسور من وضع استراتيجياتٍ أكثر فعاليةً للاستكشاف والإنتاج في مكامن الهيدروكربون.

الكلمات المفتاحية:

الكسور، علم الصخور، الدولوميت، الصخور الكربونية في العصر الجوراسيك العلوي، الستيلوليت، تطور السوائل القديمة، التشخيص الدفن الضحل والعميق

DOI: 10.33899/injes.v26i4.60916, ©Authors, 2026, College of Science, University of Mosul.

This is an open-access article under the CC BY 4.0 license (http://creativecommons.org/licenses/by/4.0/)